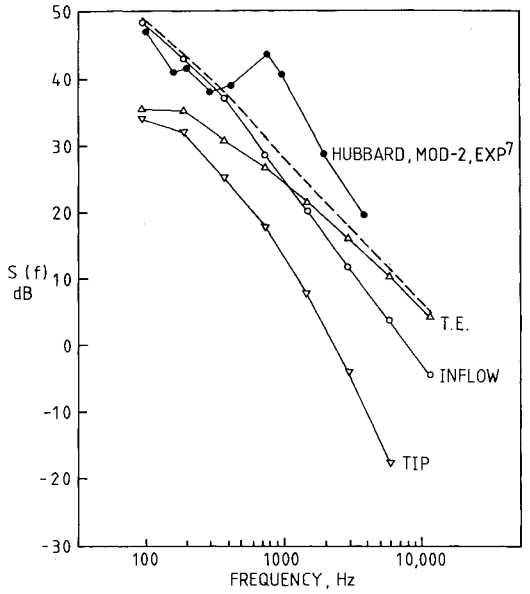

Fig. 4 Comparison of predictions with Hubbard et al.'s experiment[7] for MOD-2 wind turbine, $\Lambda = 55$ m, $\sqrt{w^2} = 1$ m/s, ground distance = 69 m.

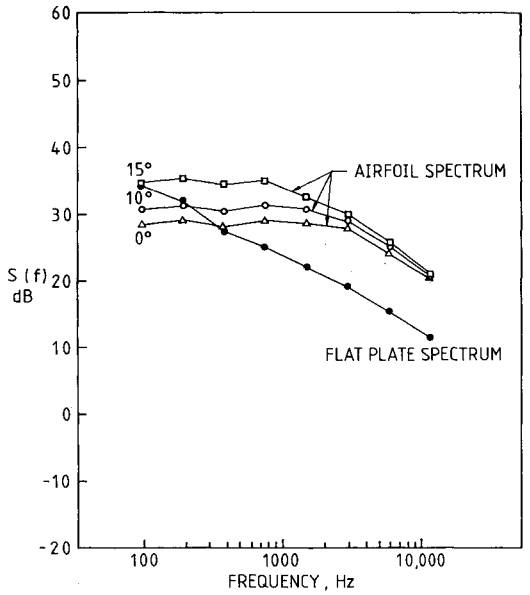

Fig. 5 Effect of rotor pitch on trailing-edge noise, UH-1, $\phi = -27$ deg.

Boundary-layer trailing-edge noise is not the only source of rotor broadband noise. Other mechanisms such as inflow turbulence and tip vortex separation also contribute significantly to the noise radiation. Thus, to evaluate the present analysis by comparing with existing experiments, one must also include other possible sources. As discussed in Ref. 1, trailing-edge noise can be important for low inflow turbulence levels or when considering a large rotor. The first experiment for comparison is an indoor model rotor test performed at the UTRC anechoic wind tunnel by Paterson and Amiet.[6] The case we picked corresponded to the no-grid case which had the lowest inflow turbulence level. Figure 3 shows the comparison. Trailing-edge noise, in this case, does not seem to be dominant in the frequency range of interest; however, it is significant and when we add up all the contributions, the result agrees very well with the experiment. The second comparison is to the MOD-2 wind turbine generator noise data of Hubbard and Shepherd.[7] Figure 4 shows the result; in this case, trailing-edge noise dominates for frequencies higher than about 1000 Hz.

Figure 5 shows the effect of angle of attack on the trailing-edge noise for a UH-1 helicopter. The result leads to a conclusion that the primary effect of angle of attack is in the low- to mid-frequency range, where the noise level increases with angle of attack. However, in the high-frequency range, the change of noise level due to change of angle of attack is not very significant. The comparison of predictions using the present analysis to that using flat plate data only[2] shows the important effect of the angle of attack on rotor trailing-edge noise.

Additional examples are given in Ref. 8.

Acknowledgments

This research was supported by NASA Langley Research Center, Dr. F. Farassat, Technical Monitor.

References

[1] George, A. R. and Chou, S.-T., "Comparison of Broadband Noise Mechanisms, Analyses, and Experiments on Rotors," *Journal of Aircraft*, Vol. 21, Aug. 1984, pp. 583-592; also AIAA Paper 83-0690, April 1983.

[2] Kim, Y. N. and George, A. R., "Trailing-Edge Noise from Hovering Rotors," American Helicopter Society Preprint 80-60; also *AIAA Journal*, Vol. 20, Sept. 1982, pp. 1167-1174.

[3] Schlinker, R. H. and Amiet, R. K., "Helicopter Rotor Trailing Edge Noise," NASA CR-3470, Nov. 1981.

[4] Yu, J. C. and Joshi, M. C., "On Sound Radiation from the Trailing Edge of an Isolated Airfoil in a Uniform Flow," AIAA Paper 79-0603, March 1979.

[5] Brooks, T. F. and Hodgson, T. H., "Prediction and Comparison of Trailing Edge Noise Using Measured Surface Pressures," AIAA Paper 80-0977, June 1980.

[6] Paterson, R. W. and Amiet, R. K., "Noise of a Model Helicopter Rotor Due to Ingestion of Turbulence," NASA CR-3213, Nov. 1979.

[7] Hubbard, H. H., Shepherd, K. P., and Grosveld, F. W., "Sound Measurements of the MOD-2 Wind Turbine Generator," NASA CR-165752, July 1981.

[8] George, A. R. and Chou, S.-T., "Broadband Rotor Noise Analysis," NASA CR-3797, April 1984.

Thermal Performance of a Logarithmic-Spiral Resonance Tube

Rafik A. Neemeh,* P. Perry Ostrowski,† and James H.T. Wu‡
Concordia University, Montreal, Canada

Introduction

THE simple Hartmann-Sprenger tube consists of a closed-end tube that is excited by an underexpanded gas jet facing its open end to produce violent, cyclic fluid oscillations internally and externally. Although this phenomenon has been known for some time, the heat generation capability of this device has been exploited only relatively recently.[1] Sprenger experimented to demonstrate that end-wall tem-

Received Dec. 12, 1983; revision received Jan. 27, 1984.

*Associate Professor, Department of Mechanical Engineering. Member AIAA.

†Research Associate, Department of Mechanical Engineering.

‡Distinguished Research Associate, Department of Mechanical Engineering. Member AIAA.

peratures well in excess of the exciting jet stagnation temperature could be achieved with a uniform tube. Although it was suspected that this temperature rise resulted from nonlinear wave motion, this was not verified until spark shadowgraphs[2] clearly showed the existence of internal traveling shock waves. Streak schlieren photography[3] has shown that these are generated during the inflow phase of each cycle and that when higher harmonics are driven, several traveling shocks are present simultaneously.

Once it was recognized that thermal effects in the simple Hartmann-Sprenger tube resulted mainly from repeated shock heating of the fluid trapped inside, it became evident that the thermal performance could be enhanced either by strengthening the internal shock or increasing the frequency of the oscillations. This may be accomplished by a variety of methods, such as minimizing the tube length, employing a light driving gas, or contouring the tube profiles to accelerate the traveling shock. Thus far, it appears that no attempt has been made to formally optimize the internal geometry in order to maximize the thermal performance; therefore, tube shapes have been selected rather arbitrarily. Tapered tubes have commonly been employed to yield end-wall temperatures as high as 725°C using air[4] and 540°C with hydrogen.[5] A cylindrical resonator that operates on a shock implosion-explosion cycle has been devised by Wu et al.[6] in order to take advantage of the significant shock amplification that may be achieved through symmetrical implosion.

The present Note investigates the thermal performance of a Hartmann-Sprenger tube with a two-dimensional logarithmic spiral internal contour. This particular profile was selected on the basis of prior shock tube studies,[7] which have shown that the shock motion in such area contractions yields cylindrical implosion and is, therefore, attractive for the present application. For experimental convenience, only two-dimensional shapes are tested, and performance is judged on the basis of spark schlieren photographs, end-wall temperatures, and piezoelectric pressure measurements.

Experiments

All tests were conducted with air as the working fluid. Flow visualization was accomplished with tubes of rectangular cross section (5.1×25.4 mm at the entrance) which were excited by an underexpanded jet from a converging nozzle with the same exit dimensions. Cavities with rectangular, 10-deg tapered, and logarithmic spiral wall contours with respective lengths of 15.2, 13.1, and 13.3 cm were tested. A single spark schlieren photograph was obtained for each test. Piezoelectric pressures were measured at different locations.

Temperature measurements were conducted with a second set of tubes, 17.8-cm long and 10.2-mm square at the entrance, whose walls were constructed with an asbestos compound. The tapered and spiral tubes have instrumentation ports 2.5-mm wide by 12.7-mm long for which chromelalumel thermocouples are located at the port midpoints. Each cavity is excited by an underexpanded air jet of diameter $d=10.2$ mm.

Results and Discussion

Spark schlieren photographs of the shock propagation in the tapered and logarithmic spiral tubes are presented in Figs. 1 and 2, respectively, for a jet pressure ratio of 1.92 and a nozzle to cavity separation $h/d=0.85$. Figure 1 is seen to be characterized by the appearance of Mach reflection due to the inclination of the channel walls, whereas Fig. 2 is observed to exhibit a curved shock normal to the wall surfaces with no reflected shocks trailing behind. Here, the shock appears to eventually collapse into a relatively small region.

Piezoelectric pressure measurements were carried out near the focus of the logarithmic spiral channel. From the recorded pressure histories, the pressure rise across the incident shock is found to increase, while that ahead of the shock decreases as the shock proceeds toward the vertex of the spiral which yields significant shock amplification. The pressure rise across the shock becomes twice that observed in the parallel tube walls. Thus, it appears that the logarithmic spiral cavity exhibits much better shock amplification than the square cavity.

The thermal performance of the three insulated tubes is shown in Fig. 3, which presents the maximum measured end-wall temperature vs jet pressure ratio. It is evident from the figure that the logarithmic spiral profile consistently achieves a higher temperature than the tapered tube over the entire range of jet pressures employed for the present tests. The increment in thermal performance is roughly constant. This implies that the shock amplification in the logarithmic spiral tube is significantly greater than in the tapered and rectangular tubes. It is evident from Fig. 3 that the peak thermal performance of the logarithmic spiral tubes employed in the present tests is rather low (320°C) compared to that obtained by other investigators,[4,5] but it is possible that higher temperatures may be achieved using a longer tube length.

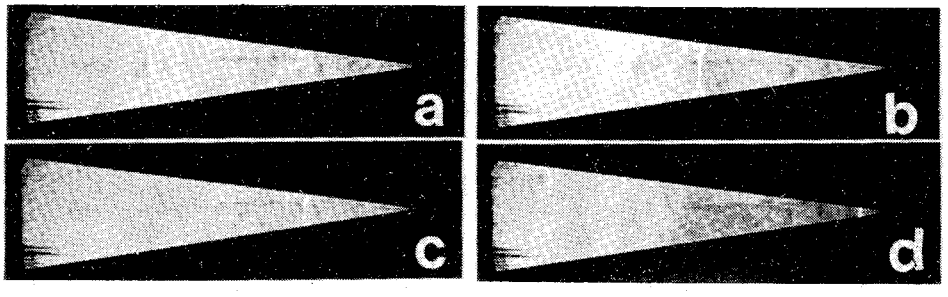

Fig. 1 Spark schlieren photographs of the shock motion within the tapered cavity, $P_{oj}/P_a=1.92$, $h/d=0.85$.

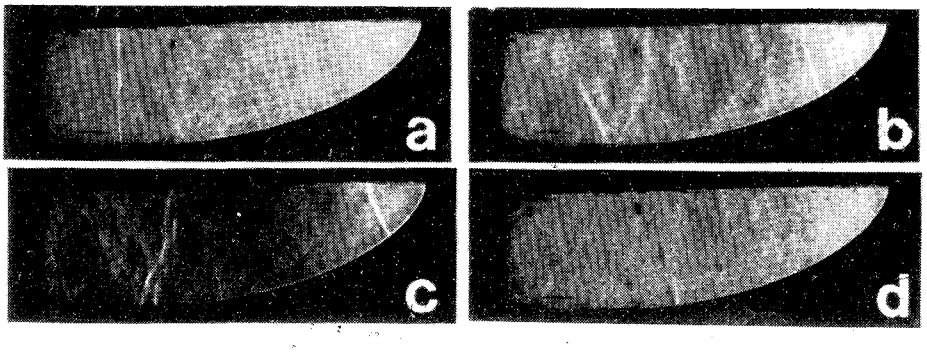

Fig. 2 Spark schlieren photographs of the shock motion within the logarithmic spiral cavity, $P_{oj}/P_a=1.92$, $h/d=0.85$.

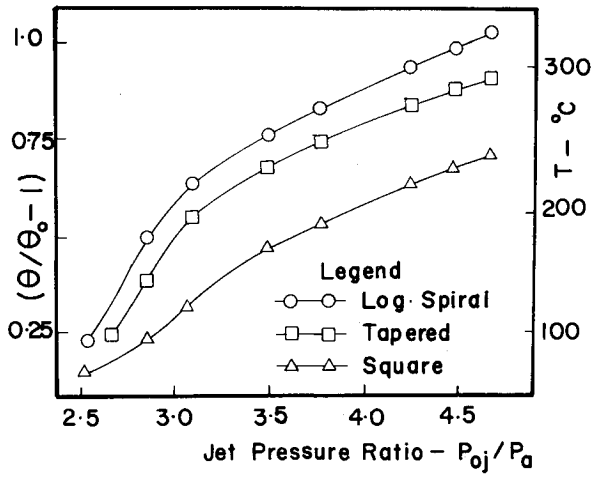

Fig. 3 End-wall temperatures.

Nevertheless, the present results are useful from a comparative rather than absolute standpoint.

Tests were also conducted to determine those locations of the tube mouth relative to the nozzle that produced maximum end-wall temperatures. Results for the logarithmic spiral profile at the jet pressure ratio of 3.77 show that the maximum temperature varies periodically with the nozzle-tube separation h due to the periodic structure of the exciting jet. The highest temperatures were recorded at $h/d = 1.7$. This means that the peak corresponds to a location where the tube mouth is situated downstream of the first pressure cell. This result differs from the findings of Przirembel and Fletcher.[8] However this difference might be explained by the fact that in their case, the open-end walls were rounded in contrast to the 30-deg chamfered entrances of the present tests.

Conclusion

Thermocouple measurements have demonstrated that a Hartmann-Sprenger tube with a logarithmic spiral profile achieves a significantly greater base temperature than a 10-deg tapered tube or a rectangular tube of comparable length. This improved performance is interpreted to result from a higher degree of shock amplification which produces a greater entropy rise in the shock-heated indigenous gas that remains trapped inside the tube. Therefore, it appears that an axisymmetric logarithmic spiral tube could be used to improve the performance further.

Acknowledgments

The work was supported by the Natural Sciences and Engineering Research Council of Canada under Grant A-4206. The assistance of M.N. Elabdin is acknowledged.

References

[1] Brocher, E., "Heat Transfer and Equilibrium Temperature Near the End Plate of a Hartmann-Sprenger Tube," *Shock Tube and Shock Wave Research,* University of Washington Press, Seattle, Wash., 1977, pp. 66-73.

[2] Hall, I.M. and Berry, C.J., "On the Heating Effect in a Resonance Tube," *Journal of the Aerospace Sciences,* Vol. 26, April 1959, p. 253.

[3] Wu, J.H.T., Neemeh, R.A., and Ostrowski, P.P., "Resonance Tubes in Underexpanded Sonic Jets," *CASI Transactions,* Vol. 6, March 1973, pp. 26-35.

[4] McAlevy, R.F. and Pavlak, A., "Tapered Resonance Tubes: Some Experiments," *AIAA Journal,* Vol. 8, March 1970, pp. 571-572.

[5] Phillips, B.R. and Pavli, A.J., "Resonance Tube Ignition of Hydrogen-Oxygen Mixtures," NASA TN D-6354, 1971.

[6] Wu, J.H.T., Ostrowski, P.P., Neemeh, R.A., and Lee, P.H.W., "Experimental Investigation of a Cylindrical Resonator," *AIAA Journal,* Vol. 12, Aug. 1974, pp. 1076-1078.

[7] Wu, J.H.T., Archer, R.D., and Molder, S.M., "Shock Propagation in a Two-Dimensional Symmetric Logarithmic Spiral Channel," *Recent Developments in Shock Tube Research,* Stanford University Press, Stanford, Calif., 1973, pp. 604-612.

[8] Przirembel, C.E.G. and Fletcher, L.S., "Aerothermodynamics of a Simple Resonance Tube," *AIAA Journal,* Vol. 15, Jan. 1977, pp. 101-104.

Proper Definition of Curvature in Nonlinear Beam Kinematics

Dewey H. Hodges*
U.S. Army Research and Technology Laboratories (AVSCOM)
Ames Research Center, Moffett Field, California

Introduction

IN the analysis of large deflections of beams, it is important to include effects of geometric nonlinearity. Sometimes the nonlinear curvature expressions used in published works are incorrect and the reasons why may appear subtle. The purpose of this Note is to show why the curvature expression in the typical calculus text is not always appropriate for the kinematics of a deformed beam. To illustrate this, a relatively simple example involving the kinematics of a beam deforming in a plane is used. No attempt is made here to cite all the references pertinent to this subject. Neither is there an attempt to present a new development; the main motivation is tutorial.

Development of Equations

The development herein is similar to a more general one found in Ref. 1. Consider a beam with coordinate systems, as shown in Fig. 1. For purposes of discussion, the neutral axis of the undeformed beam lies along the x axis and the y axis is normal to the x axis at the root end of the beam denoted by E. The x and y axes are fixed in space. The position of a material point M relative to E in the beam prior to deformation is given by

$$\underline{R}^{ME}|_{\text{undeformed}} = x\underline{e}_x + y\underline{e}_y \tag{1}$$

where $\underline{e}_x$ and $\underline{e}_y$ are unit vectors along the x and y axes, respectively. It is assumed that a set of material points at $x = \text{const}$, in a plane prior to deformation, remain in a plane during deformation. Furthermore, the cross section is assumed not to deform in its plane. Then, as usual for a Lagrangian procedure, the beam's geometry during deformation can be characterized by the unknown functions $u(x)$, $v(x)$, and $\zeta(x)$ so that the same material point M has location relative to E during deformation given by

$$\underline{R}^{ME} = (x+u)\underline{e}_x + v\underline{e}_y + y\underline{e}_\eta \tag{2}$$

where $\underline{e}_\eta$ is a unit vector in the plane of the cross section during deformation. Another important unit vector is $\underline{e}_\xi$,

Received Aug. 17, 1983; revision received Jan. 15, 1984. This paper is declared a work of the U.S. Government and therefore in the public domain.

*Research Scientist and Theoretical Group Leader, Rotorcraft Dynamics Division, Aeromechanics Laboratory, Associate Fellow, AIAA.